

Anomaly Detection in Energy Usage Patterns

Henry Linder¹, Nalini Ravishanker^{1,*}, Ming-Hui Chen¹, David McIntosh²,
and Stanley Nolan²

¹Department of Statistics, University of Connecticut, Storrs, CT 06269

²Utility Operations & Energy Management, Facilities Operations,
University of Connecticut, Storrs, CT 06269

*Corresponding author: nalini.ravishanker@uconn.edu

Abstract

Energy usage monitoring on higher education campuses is an important step for providing satisfactory service, lowering costs and supporting the move to green energy. We present a collaboration between the Department of Statistics and Facilities Operations at an R1 research university to develop statistically based approaches for monitoring monthly energy usage and proportional yearly usage for several hundred utility accounts on campus. We compare the interpretability and power of model-free and model-based methods for detection of anomalous energy usage patterns in statistically similar groups of accounts. Ongoing conversation between the academic and operations teams enhances the practical utility of the project and enables implementation for the university. Our work highlights an application of thoughtful and continuing collaborative analysis using easy-to-understand statistical principles for real-world deployment.

Keywords: Boxplots, Cluster analysis, Graphical interface, Proportions, Utility Management.

1 Introduction

Energy management at large academic institutions usually poses unique operational challenges (Cruz Rios et al., 2017). The energy infrastructure in a university can be complex across multiple dimensions: the number of buildings at a campus is large, the facilities exhibit diverse use-types, and the buildings vary in size, energy efficiency, and state of repair. For utility managers, close and in-depth scrutiny of energy usage across the entire campus must be balanced against time and manpower by using resources for the most critical maintenance problems. The balance between these priorities is the focus of Facilities Operations in an institution. Understanding and monitoring patterns in historical energy usage data and identifying anomalous behavior is an important step in this direction, and statistical methods can provide a systematic framework for implementing these.

This is the focus of an ongoing collaboration at the University of Connecticut between the Department of Statistics and Facilities Operations - for working together in a concerted way to achieve systematic and statistically valid procedures to understand patterns and detect anomalies in energy usage, ultimately minimizing wasteful consumption. We describe the problem of managing and monitoring monthly energy usage in a large set of utility accounts located across the university's 4000 acre main campus. The number of accounts is prohibitively large to permit manual assessment by Facilities Operations engineers. Moreover, while each account individually represents only a small fraction of overall energy consumption on campus, nonetheless, when aggregated across several hundred accounts over the full fiscal year, abnormal consumption may pose a substantial financial cost for the university. Since energy use is a fundamental need for university operations, the mandate from Facilities Operations is to statistically distinguish abnormal and unnecessary usage from anticipated and essential usage. We do an in-depth analysis of time series of *monthly* energy usage, as well as monthly proportions within each year of the energy usage. We have chosen to employ simple, but effective statistical procedures that can be easily communicated to engineers and be jointly implemented with our collaborators from Facilities Operations on ready-to-use dashboards. The variety of building use-types on the university campus poses a unique challenge. An individual building's energy consumption profile depends directly on factors including use-type, square footage and building age.

There also exists significant correlations between energy usage on different campus buildings due to common drivers such as student and faculty population sizes, climate variations within a year, and campus-wide energy initiatives.

Existing literature on methods for visualizing campus energy usage and understanding and modeling energy data varies in the level of detail and sophistication. Students at the Worcester Polytechnic Institute (O’Hara et al., 2020) discussed the physical infrastructure needs for real-time collection of electricity data, with a focus on the hardware metering technology used to measure demand. The Harvard Medical School implemented a real-time visualization dashboard for energy usage by building (Lieberman, 2010) to present graphics of historic energy usage, with a goal of increasing community awareness. Breyer et al. (2020) considered software solutions to encourage behavioral changes in campus energy consumers at the University of Michigan. They focused on public-facing tools to increase awareness among student, faculty, and staff communities to achieve structural changes in demand for energy. Ma et al. (2015) gave a descriptive analysis of aggregate energy consumption at seven universities across the world. They considered the effects of population and building footprint size on energy consumption, and used this to compare an energy consumption index between universities to assess their relative energy usage.

To our knowledge, existing literature on anomaly detection methods for energy consumption seem to primarily focus on high-frequency demand/usage data which are not suitable for coarser-grained monthly data. The methods used in these papers ranged from using z -scores relating the mean and standard deviation for individual time series based on previous behavior (Seem, 2007) to looking for or large discontinuities in usage (Zhao, 2014) to using reduced dimension processes and looking for large prediction errors (Ma et al., 2017) or distance based abnormality scores (Rashid and Singh, 2018).

The literature does not address statistical concepts such as power of the anomaly detection schemes or the probability of false positives, nor the mechanisms for anomaly detection in monthly proportions data. It also does not directly address the managerial problem of monitoring a large number of energy accounts, observed at a low frequency and with small sample sizes. Many existing methods are intended for monitoring a small number of high-frequency time series, but that type of data is only available for a small subset of buildings.

Moreover, the Facilities Operations management problem exists even when high-frequency meter data is unavailable, so small data approaches are still necessary.

In this article, we describe our collaborative work with Facilities Operations which highlights the value of statistical practice by academics that focuses on operational problem-solving. To identify candidate buildings that may exhibit aberrant energy usage, we consider energy consumption across the fiscal year. We also integrate data from external sources to normalize usage by relevant weather covariates, and then convert these into monthly usage proportions within the year. We group buildings according to similar characteristics, and apply statistical clustering methods. This enables full utilization of the similarities in consumption profiles across accounts. By grouping buildings with similar energy consumption profiles, we obtain an aggregate benchmark against which we assess the usage characteristics of individual accounts within these buildings. We propose a graphical, model-free method for anomaly detection based on approximate, group-wise control limits on boxplots constructed for transformed monthly usage proportions data. We also propose an approach based on a linear model, which we use as a benchmark against which to compare our graphical method. Our model is motivated by a statistical process control approach described by Fu and Jeske (2014). They used historical in-control data to estimate nuisance parameters in their model, leading to an approximate Bartlett-type likelihood ratio (ABLR). We report to Facilities Operations engineers a list of accounts flagged as potential outliers. These anomalies can be investigated by Facilities Operations on an ongoing basis for physical malfunctions or other maintenance problems.^a

The format of the article follows. We first provide a description of a monthly gas consumption data set collected by Facilities Operations in Section 2. In Section 3, we analyze monthly proportional usage within a fiscal year. In Section 4, we identify anomalous accounts within known homogeneous groups, using two approaches. First, we consider a model-free approach based on the boxplot to identify energy accounts that are anomalous relative to similar accounts. In Section 4.3, we introduce a model-based approach to identify changes in mean value, and compare its properties to those of the less sophisticated, model-free method. In Section 5, we describe an extension to the setting where the groups that partition accounts are not all known *a priori* and must be statistically determined.

Finally, we end in Section 6 with a discussion of the interface that we provide to Facilities Operations.

2 Data Description

The raw data consist of monthly measurements of natural gas consumption collected by Utility Operations and Energy Management in Facilities Operations at the university’s main campus. A total of 245 separate utility accounts are available across 115 buildings, with the number of accounts varying between buildings. In some cases one building contains multiple accounts, such as an apartment building with several units. In what follows, we have denoted buildings by generic names due to privacy considerations.

The availability of historical data varies by building and account, with the earliest observation in February 2007 and the last in December 2018. Prior to the analysis, we omitted four accounts which have missing final observations, as this is an indication that the accounts are no longer actively used. We also omitted 1 account with over 10% of observations missing, and 2 other accounts known *a priori* to be substantial outliers. Table 1 shows the time series lengths in our dataset, most of which are either 82 or 143 months long. For example, of the 71 accounts in Apartment Complex A, 69 series were observed from February 2007, or for 143 months; 1 series for 137 months; and the last for only 82 months.

Year	Month	Freq.	Year	Month	Freq.
2007	February	128	2011	March	3
2007	May	1	2011	April	2
2007	August	1	2011	June	1
2008	May	1	2011	July	2
2009	April	1	2012	March	83
2009	December	1	2013	March	1
2010	March	3	2013	May	1
2010	April	1	2015	January	3
2010	September	1	2015	April	2
2010	October	1	2016	June	1

Table 1: Series start dates with observed frequencies. Values count the series beginning in a given month.

For the 238 accounts used in the analysis, monthly gas consumption was measured in units of hundred cubic feet (“CCF”). Each observation corresponds to a single utility bill in one account in one billing period, measured as the difference between two meter readings. The bills are grouped across accounts by a calendar-monthly billing period. The billing period provides a reference alignment of each utility bill, despite differences across accounts in the specific start and end dates in a given billing period. The monthly observations for two distinct residential complexes are shown in Figure 1(a). Specifically, five accounts in Apartment Complex A, Building C, and 12 accounts from Apartment Complex B are shown.

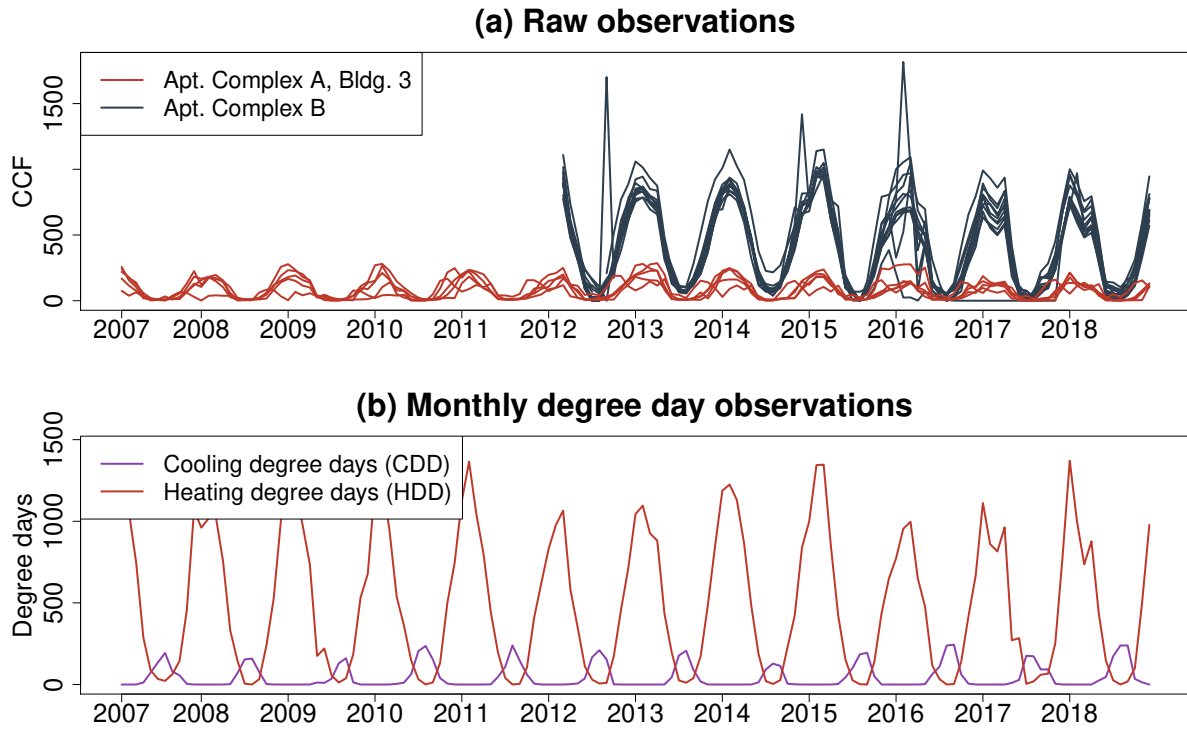


Figure 1: (a) Raw data observed in Building C of Apartment Complex A (red lines), and all of Apartment Complex B (black). Data in Complex A is available since 2007, compared with 2012 for Complex B. (b) Historical degree day observations, by heating and cooling

It is possible that a value in any month for any account may be exactly 0, for one of two reasons. First, a building may be unoccupied or otherwise inactive for that month. For instance, Apartment Complex A, Building 6, has values of 0 in the same months across several years, July and August. This is because the residence hall is unoccupied in the

summer. Second, the gas utility company only charges for integer-valued CCF values, so that a recorded value of 0 may actually represent a nonzero CCF value that is below 1.

In addition to energy usage, our analysis also includes weather covariates. We used daily weather data from the National Oceanic and Atmospheric Administration (NOAA). This data is made available through the Applied Climate Information System (<http://www.rcc-acis.org/>) web API. Based on guidance from Facilities Operations, we obtained daily observations of heating degree days (HDD) and cooling degree days (CDD) defined as

$$\text{HDD} = \max(0, 65 - \bar{u}), \text{ and } \text{CDD} = \max(0, \bar{u} - 65), \quad (1)$$

where \bar{u} refers to the average (of the maximum and minimum temperatures) on any given day. Degree days provide a nonlinear measure of temperature deviation from a neutral balance point (65 degrees), and provide a robust context for temperature (Quayle and Diaz, 1980). It is worth noting that the daily value of a single degree day will generally be greater than 1. The degree day converts the one-day deviation from the balance point \bar{u} , to \bar{u} days of 1-degree deviation from the balance point. Therefore, the degree day measures the magnitude of a deviation from the balance point. To reckon the HDD (CDD) for a month, it is usual to sum the daily HDD values. Figure 1(b) shows the historical observations of heating and cooling degree days.

In addition to the different number of calendar days in each month, the specific start and end dates for energy consumption within any month are not consistent across all accounts. We re-normalized the energy data to account for this problem in Section 3.1. We also adjusted for weather effects.

3 Processing Data and Grouping Accounts

3.1 Re-Normalization and Weather Adjustment of Data

We calculated the average consumption per day for each observation, and then re-normalized all observations to represent a 30-day month. Furthermore, we applied a standard adjustment by dividing the CCF value by the area of the building (square footage), so that each observation represents the monthly average-per-square-foot for a 30-day month. For

buildings that contain multiple accounts, we subdivided the square footage evenly across all accounts. For example, Apartment Complex A, Building C, has an area of 4521 square feet, and five gas accounts. Suppose the utility bill for one of these five accounts from 2007-01-19 to 2007-02-20 (for 32 days) is 76 CCF. We computed its normalized consumption value for February of 2007 to be: $30 \times \frac{76}{32 \times 4521/5} = 0.07880$. Figure 2(a) shows the normalized data measured in 30-day CCF per square foot. This re-normalization alleviates the issue of comparisons between months of different lengths.

We aggregated the weather covariates across all days of the billing period and then summarized within that period. Therefore, the weather covariates may vary, even for observations with the same nominal billing period, if the meters were observed across separate days. Then, we additionally adjusted the observations by dividing the normalized values by the sum of the HDD and CDD in the corresponding month. We used these adjusted observations for our analysis.

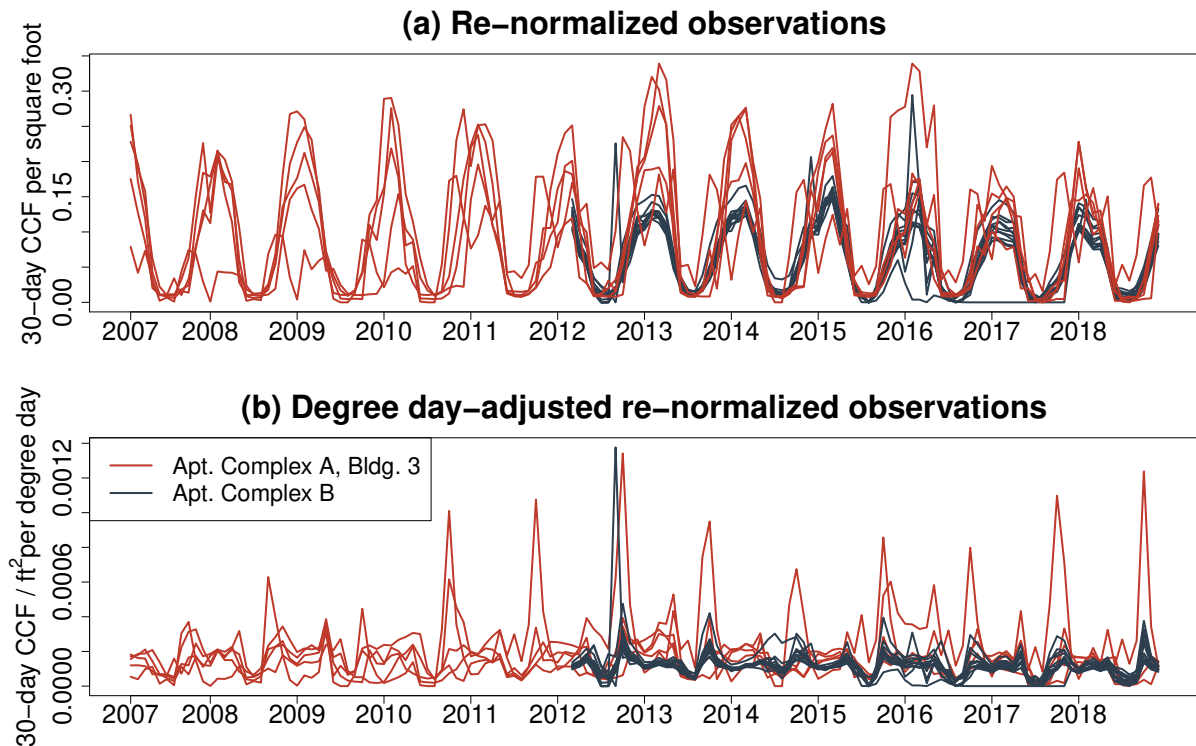


Figure 2: (a) Normalized data, adjusted for nominal month billing period duration and per-unit square footage. (b) Degree day-adjusted re-normalized data, with imputed values.

3.2 Missing Data Imputation

Of the 238 accounts, 39 accounts have missing observations in the time series interior. The number of missing values in any of the 39 time series was at most 7, while 23 series only had missing a single value. We believe that it is reasonable to assume that these values are missing at random, as they typically arise from clerical oversight (Little and Rubin, 2019). We used the “imputeTS” package in R (Moritz and Bartz-Beielstein, 2017) to impute the missing values in the degree day-adjusted re-normalized observations. Based on a visual inspection of the output of the various interpolation, Kalman smoothing, and moving average options in this package, we selected the *Kalman smoothing and structural time series model* option. We note that, if an imputed value was negative, we replaced the imputed value with 0 (since consumption must be non-negative). The weather-adjusted re-normalized series with imputed values are shown in Figure 2(b).

3.3 Grouping of Accounts

Table 2 gives the number of accounts (each corresponding to a monthly time series) for the seven utility services.

Utility Service Type	Service Group	# of Accounts
Non-Residential Small General Service	Small non-residential	108
Non-Residential Medium General Service	Medium to large non-residential	33
Non-Residential Large General Service	Medium to large non-residential	1
Seasonal - Commercial	Medium to large non-residential	1
Residential Heating	Residential	74
Residential Multi-dwelling Large	Residential	9
Residential Multi-dwelling Small	Residential	1

Table 2: Frequency distribution of accounts by utility service types. By merging several service types, we formed three service groups.

This classification reflects real-world groupings of the buildings and accounts, including residential housing, academic and administrative buildings, food service locations, and agricultural support buildings. Different building use-types exhibit different consumption profiles. Broadly speaking, we expect accounts with shared physical or functional characteristics to exhibit similar consumption based on their use-types. We use the service groups

given in Table 2 to form three homogeneous groups of accounts: small non-residential; medium to large non-residential; and residential.

We illustrate this for undergraduate housing in Apartment Complex A. Each unit occupies approximately 1000 square feet. Removing accounts with missing values, we observe $N_1 = 70$ accounts. The re-normalized data for these accounts are shown in the top of Figure 3. The pattern of these time series reflects the use of gas for heating in the winter. The accounts after degree day adjustment are shown in the bottom panel of Figure 3.

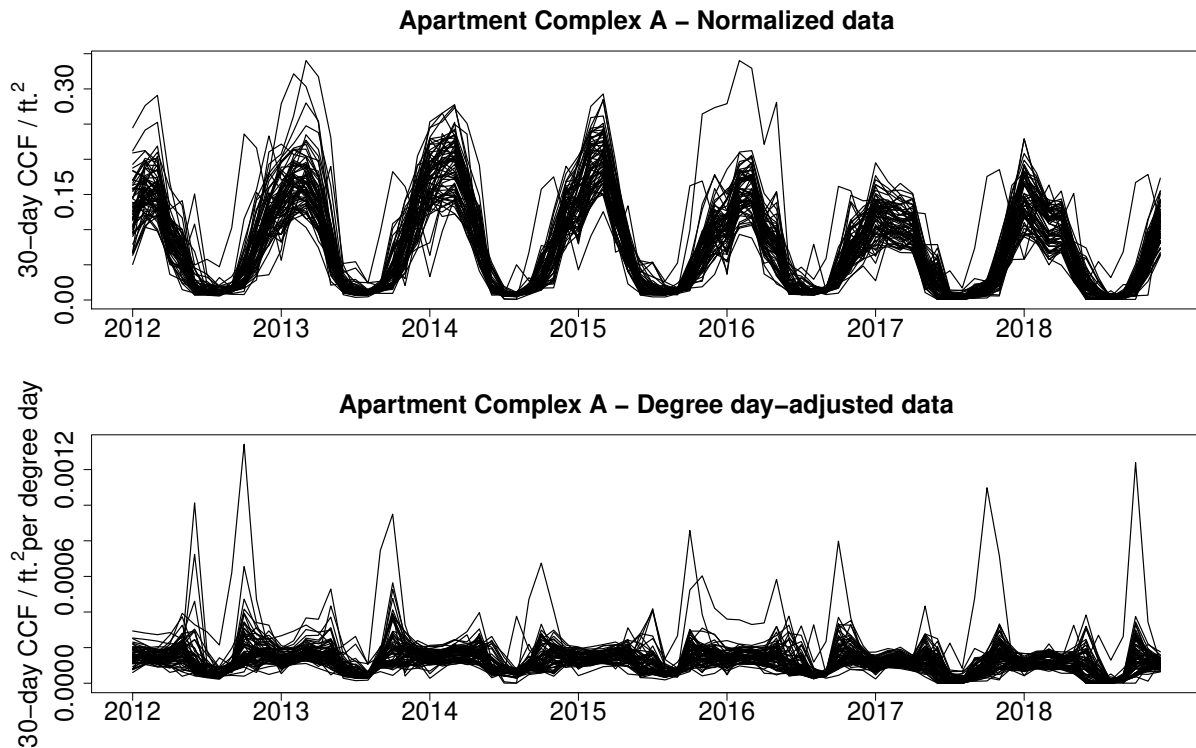


Figure 3: Historical data for 70 gas accounts in Apartment Complex A. *Top*: Normalized data, calculated as hundred cubic feet (CCF) per square foot, averaged over billing period duration and aggregated to a 30-day month. *Bottom*: Degree day-adjusted and normalized data, calculated as per-degree day, where degree days are the sum of cooling and heating degree days.

We grouped the data into yearly cycles based on the university’s fiscal year, which begins on July 1 and continues until the following June 30. This grouping coincides with both the university’s accounting schedule and the academic year. Student residents depart campus in May, so logistically, summer is a good time for Facilities Operations to address maintenance problems.

4 Detecting Anomalies in Accounts from Known Homogeneous Groups

4.1 Model-Free Anomaly Detection on Adjusted Usage Data

Anomaly detection could refer to identifying an account with behavior that departs markedly from its own history, or from a normal pattern that is expected based on known characteristics for that account. For example, the normal pattern for each month could be represented by a median, or suitable quantiles of the expected usage of the accounts.

Based on observations from all 70 accounts in Apartment Complex A, we applied a moving window of two years and computed curves that represent the 2.5% and 97.5% percentiles across both years. We then considered using the curves as reference limits for normal behavior in the following year. Our choice to use a two year window was motivated by the high degree of variance we observed in the quantiles when considering quantiles for only the single preceding year.

We show six years (2012 to 2018) of weather-adjusted data in Figure 4, and the quantiles for the previous two years are shown in red. Our intention was to use the quantiles to identify accounts with an anomaly in some month, identified by a usage value falling outside the reference quantiles. The two year window accommodates systematic structural changes to the consumption pattern over time. This tendency is apparent in the shift of peak consumption from October in 2012–2013, to November in 2017–2018.

The reference quantiles derived from the previous two years represent aggregates across multiple accounts. For a specific building, deviations from those reference quantiles will be due to idiosyncratic factors of the new year: new occupants in a dormitory, new class schedules in academic buildings. Therefore, they may be assumed to be statistically independent of observations in the current year. We used this to directly flag outlying values in. Below the horizontal axis of each panel of Figure 4, we report the number of accounts above and below the reference quantiles.

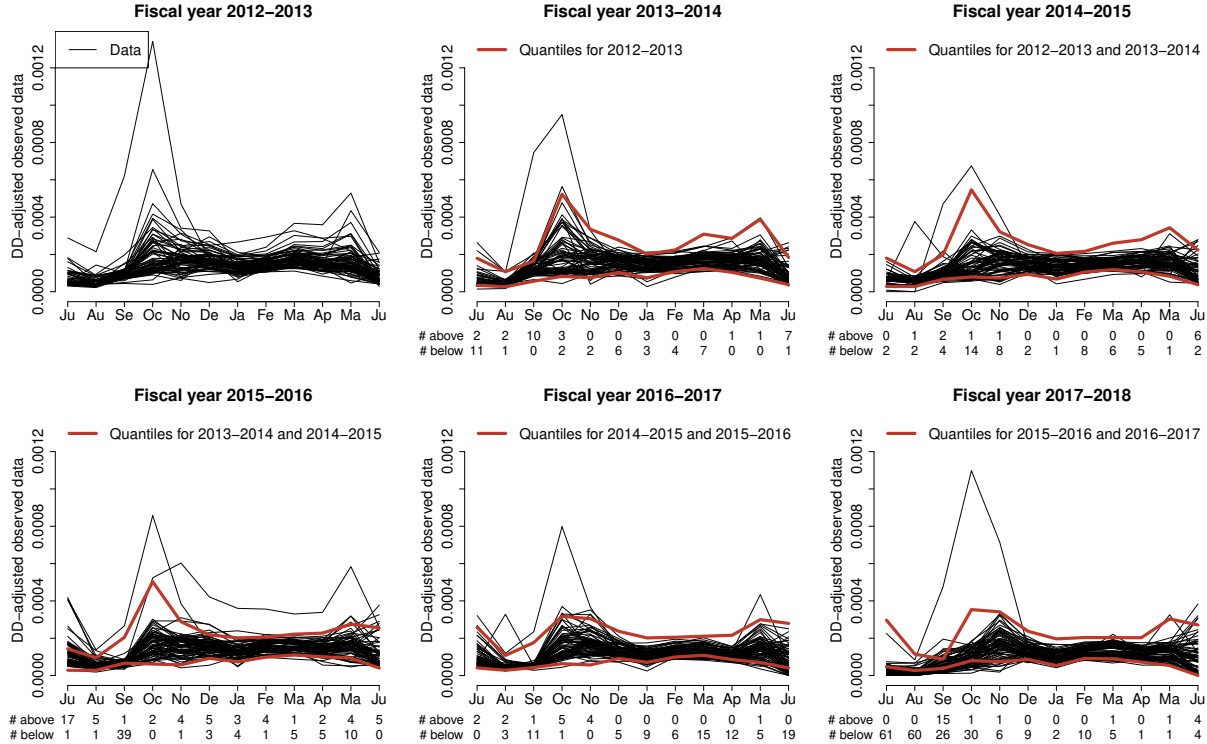


Figure 4: Fiscal year observations for Apartment Complex A. Red lines give previous two years’ 2.5% and 97.5% quantiles. Below the chart is the number of accounts above the 97.5% quantile (line 1) and below the 2.5% quantile (line 2).

The reference quantiles captured the dominant central tendency of recent observations. This permits identification of anomalous accounts such as in 2015–2016, where a single account is consistently elevated above other series. This demonstrates the importance of grouping together buildings with similar consumption profiles: for a different building use-type, that series might not be anomalous. On the other hand, we flag a large number of accounts as “outliers” from July to October in 2017. This suggests that the accounts we flagged might not provide a meaningful summary of deviation from a “normal” baseline. In particular, the past quantiles do not reflect behavior in the current year.

Another important aspect of Figure 4 is the recurrence of level differences across accounts. This is apparent in the series with repeatedly high usage in October. Because the magnitude of this series dominates the other series, it is difficult to compare this series with the others. This may reflect a systematic difference in that account, but it also suggests that level shifts may pose an obstacle to applying these quantiles to the data.

4.2 Model-Free Anomaly Detection on Proportions

We identified two problems with the quantile-based flagging, namely, (1) inconsistent usage patterns from one year to the next, despite within-group homogeneity in a single year; and (2) differences in scale that may dominate usage patterns that are otherwise similar. To remedy these problems, we calculated proportional usage for each month within the fiscal year. Denoting energy usage in a given year for account i in month m by x_{im} , $i = 1, \dots, N$, where $N = 70$, $m = 1, \dots, 12$, we computed the proportion p_{im} of usage in month m relative to overall consumption:

$$p_{im} = x_{im} / \sum_{k=1}^{12} x_{ik} \quad (2)$$

The resulting sequence is of length 12.

The proportion transformation permits us to compare accounts with different magnitudes by removing level information about the series. It also allows us to address the variability in usage patterns between years, such as the shift of peak usage from October to November noted above in Section 4.1. This is accomplished by summarizing the relative magnitude of each month’s observation, while also controlling for year-wide changes in temperature allocation, occupancy of residences, and other factors that may vary from year to year.

We considered applying Tukey’s boxplot to the marginal monthly proportions across all accounts. The boxplot defines a convenient definition of an outlier, defined in terms of individual observations from a homogeneous group. Denote the lower and upper quartiles of the data (25% and 75% quantiles, respectively) by Q_1 and Q_3 . The interquartile range is defined as $\text{IQR} = (Q_3 - Q_1)$, which is a robust estimate of the population variance.

Tukey’s thresholds for outliers are based on the lower and upper fences, which are defined in Table 3 for moderate and severe outliers. The lower bound for non-outlier values is found as the smallest observed value larger than the lower fence. Likewise, the upper bound is the largest observed value smaller than the upper fence.

These threshold bounds assume a normally-distributed sample, which is clearly violated by proportion values. Therefore, we transformed each proportion to the logit scale, defined

	Moderate outlier	Severe outlier
Lower fence	$Q_1 - 1.5 \times \text{IQR}$	$Q_1 - 3 \times \text{IQR}$
Upper fence	$Q_3 + 1.5 \times \text{IQR}$	$Q_3 + 3 \times \text{IQR}$

Table 3: Lower and upper fences for outlier detection, based on Tukey’s boxplot. The lower bound is the smallest value larger than the lower fence, and the upper bound is the largest value smaller than the upper fence. Observations below the lower bound or above the upper bound are flagged as outliers.

by the transformation

$$\ell_{im} = \log\left(\frac{p_{im}}{1 - p_{im}}\right) \quad (3)$$

We then constructed boxplots within each month across all accounts. These boxplots are shown for three fiscal years in the top panel of Figure 5.

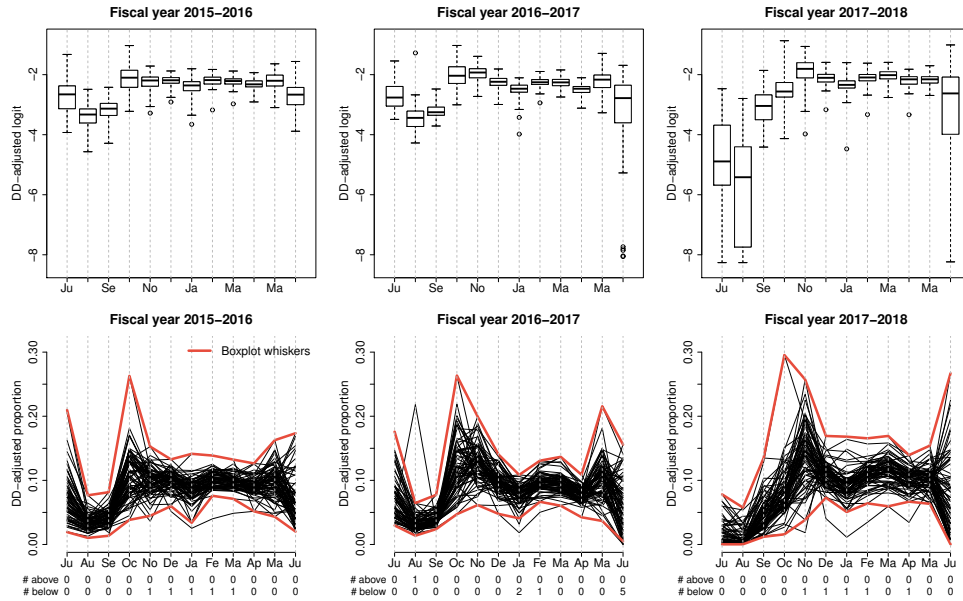


Figure 5: Boxplots on logit of monthly proportions of fiscal yearly consumption (top), and corresponding proportions (bottom). Bounds corresponding to the boxplot whiskers are shown in red.

The number of outliers is marked below the bottom panel of Figure 5. The boxplots identify two of the residential accounts as outliers in fiscal year 2017–2018. The proportions for these series are highlighted in Figure 6. One of the accounts exhibits elevated usage in

October relative to other accounts in the group, and relatively low usage from December to April. The decrease exhibits the outliers, although the specific decreases in the proportions may be due to a linear response to the exceptionally large usage in October. The other series exhibits low usage in November, and relatively high usage from December to March. The outlier data point itself is the low usage in November, and the elevated usage in the winter does not register as statistically significant. The proportions clearly demonstrate lower consumption in some months, although these same points appear far less abnormal in the non-proportion data.

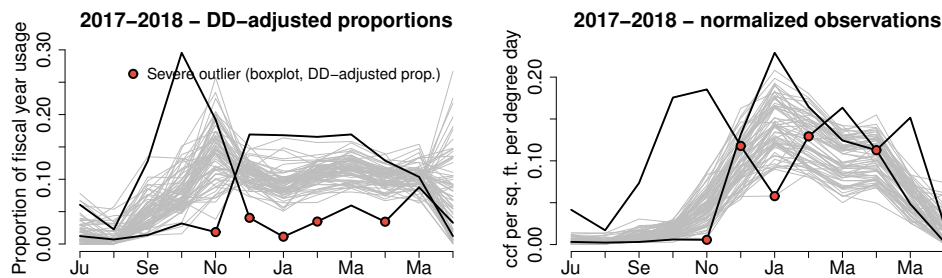


Figure 6: Outlier observations from 2017–2018. Proportion data is shown at left, degree-day-adjusted data on the right. Series with outliers are highlighted, and outlier observations are marked.

We follow in detail the historical paths of these two accounts in Figure 7. In previous years, we observe that the behavior of Account 2 is comparable to the other accounts in Apartment Complex A, with a marked change in 2017–2018. In contrast, the large value in Account 1 recurs with the same pattern across years, and is consistently out-of-sync with the other buildings. Further investigation revealed that Account 1 is the only account in Apartment Complex A that is classified by the utility as “non-residential small general service”, instead of “residential heating.” Moreover, a Facilities Operations annotation for this account indicates this account is used for the laundry dryer in Building C.

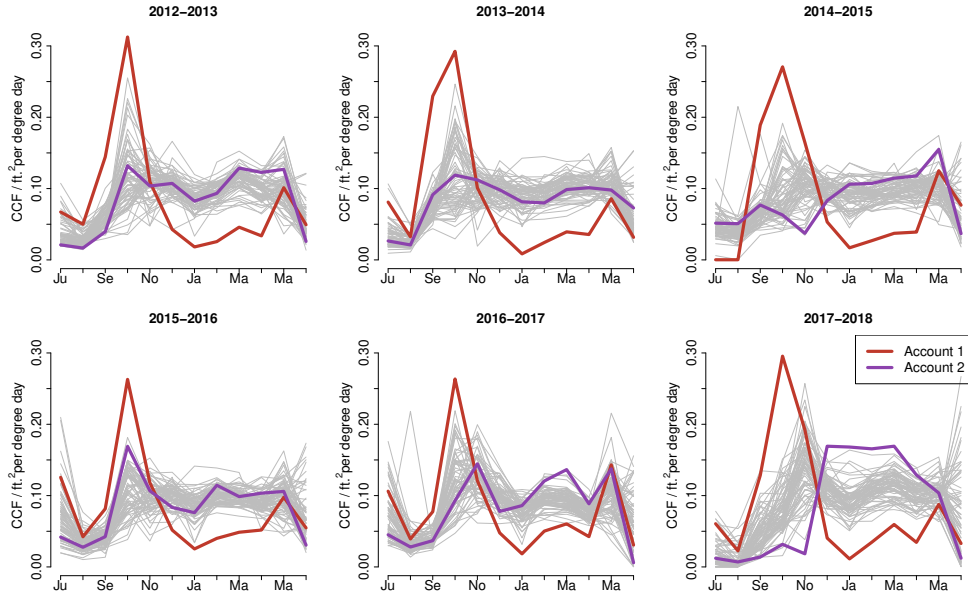


Figure 7: Outlier time series from fiscal year 2017–2018.

Therefore, we understand Account 1 to represent behavior that is truly outlying, relative to the other accounts, because we may attribute differences in consumption to known external factors. We thus conjecture that there may be a real anomaly in Account 2, as well, because of incompatibility with its own past behavior, as well as the extreme low consumption in November. Further investigation by Facilities Operations will clarify the status of this account, and assess the reality of any anomaly there.

4.3 Model-Based Anomaly Detection on Proportions

In light of the lack of publications that consider anomaly detection on proportions, we propose a linear model that offers an approach to monitor each new observation as it arrives, in an online fashion. We adapt the general monitoring framework of Fu and Jeske (2014), which implements hypothesis tests to monitor for mean changes of a given magnitude. These authors developed an integrated likelihood ratio (ILR) test to implement a procedure similar to Bartlett’s sequential probability ratio test (SPRT). Since a “Bartlett-type likelihood ratio” (BLR) test would require multivariate integration across many dimensions as well as a maximization over nuisance parameters, they instead used historical in-control data to estimate the nuisance parameters, leading to an approximate Bartlett-type likeli-

hood ratio (ABLR).

As above, we consider observations of monthly energy consumption data for N utility accounts. We further consider K historical years of data, and modify our notation accordingly. Denote the consumption in month m of year k for the i th account by x_{ikm} , $i = 1, \dots, N$, $k = 1, \dots, K$, and $m = 1, \dots, 12$. The dataset contains $12KN$ observations.

Each year of data is a 12-month cycle for each account. For each month m in year k for the i th account, we calculate the proportion of overall yearly consumption by

$$p_{ikm} = \frac{x_{ikm}}{\sum_{\ell=1}^{12} x_{ik\ell}}. \quad (4)$$

Finally, we apply the logistic transformation to p_{ikm} , $m = 1, \dots, 12$, yielding data

$$y_{ikm} = \log \left(\frac{p_{ikm}}{1 - p_{ikm}} \right). \quad (5)$$

Let $\mathbf{y}_{ik} = (y_{ik1}, \dots, y_{ik12})'$ denote the 12-dimensional vector of logit-transformed, yearly proportional consumptions. We assume

$$\mathbf{y}_{ik} = \boldsymbol{\beta}_i + \boldsymbol{\epsilon}_{ik}, \quad (6)$$

$$\boldsymbol{\epsilon}_{ik} = (\epsilon_{ik1}, \dots, \epsilon_{ik12})' \sim N(\mathbf{0}, \Sigma), \quad (7)$$

where $\boldsymbol{\beta}_i = (\beta_{i1}, \dots, \beta_{i12})'$ is the mean of the logit transformed yearly proportional consumptions for the i th account for $i = 1, \dots, N$.

Let $D_K = \{\mathbf{y}_{ik}, i = 1, \dots, N, k = 1, \dots, K\}$ denote the ‘‘historical’’ data for these N accounts. Write $\boldsymbol{\beta} = (\boldsymbol{\beta}'_1, \dots, \boldsymbol{\beta}'_N)'$. The likelihood function based on D_K is

$$\mathcal{L}(\boldsymbol{\beta}, \Sigma | D_K) \propto |\Sigma|^{-KN/2} \exp \left\{ -\frac{1}{2} \sum_{k=1}^K \sum_{i=1}^N (\mathbf{y}_{ik} - \boldsymbol{\beta}_i)' \Sigma^{-1} (\mathbf{y}_{ik} - \boldsymbol{\beta}_i) \right\}. \quad (8)$$

Then, the maximum likelihood estimates of β_1, \dots, β_N , and Σ are

$$\hat{\beta}_i = \frac{1}{K} \sum_{k=1}^K \mathbf{y}_{ik}, \quad i = 1, \dots, N \quad (9)$$

$$\hat{\Sigma} = \frac{1}{NK} \sum_{i=1}^N \sum_{k=1}^K (\mathbf{y}_{ik} - \hat{\beta}_i)(\mathbf{y}_{ik} - \hat{\beta}_i)'. \quad (10)$$

Let $\mathbf{y}_{K+1} = (\mathbf{y}'_{1,K+1}, \dots, \mathbf{y}'_{N,K+1})'$ denote the logit transformed yearly proportional consumptions of N accounts at year $K + 1$. Let $C = \text{diag}(c_1, c_2, \dots, c_{12})$ be a fixed 12×12 diagonal matrix such that $C \neq I_{12}$, where I_{12} is the 12×12 identity matrix. Here the values of the diagonal elements of C specify the magnitudes of change in β_i that indicate the underlying consumption is no longer in-control for the i th account. In other words, we test the hypothesis

$$H_0 : \beta_i = \beta_i^{(0)} \quad \text{vs.} \quad H_1 : \beta_i = C\beta_i^{(0)} \quad (11)$$

as we observe the new value of $\mathbf{y}_{i,K+1}$ for $i = 1, \dots, N$.

The test statistic is

$$T_i^{ABLR} = \frac{\exp \left\{ -\frac{1}{2}(\mathbf{y}_{i,K+1} - C\beta_i^{(0)})'\Sigma^{-1}(\mathbf{y}_{i,K+1} - C\beta_i^{(0)}) \right\}}{\exp \left\{ -\frac{1}{2}(\mathbf{y}_{i,K+1} - \beta_i^{(0)})'\Sigma^{-1}(\mathbf{y}_{i,K+1} - \beta_i^{(0)}) \right\}}$$

and

$$\log \left(T_i^{ABLR} \right) = (\beta_i^{(0)})'(C - I_{12})\Sigma^{-1}\mathbf{y}_{i,K+1} - \frac{1}{2}(\beta_i^{(0)})'C\Sigma^{-1}C\beta_i^{(0)} + \frac{1}{2}(\beta_i^{(0)})'\Sigma^{-1}\beta_i^{(0)}.$$

Under H_0 , we have

$$\begin{aligned} & \log \left(T_i^{ABLR} \right) \\ & \sim N \left((\beta_i^{(0)})'(C - I_{12})\Sigma^{-1}\beta_i^{(0)} - \frac{1}{2}(\beta_i^{(0)})'C\Sigma^{-1}C\beta_i^{(0)} + \frac{1}{2}(\beta_i^{(0)})'\Sigma^{-1}\beta_i^{(0)}, \right. \\ & \quad \left. (\beta_i^{(0)})'(C - I_{12})\Sigma^{-1}(C - I_{12})\beta_i^{(0)} \right). \end{aligned} \quad (12)$$

Write

$$Z_i(\mathbf{y}_{i,K+1}, \boldsymbol{\beta}_i^{(0)}, \Sigma) = \frac{\left| (\boldsymbol{\beta}_i^{(0)})'(C - I_{12})\Sigma^{-1}\mathbf{y}_{i,K+1} - (\boldsymbol{\beta}_i^{(0)})'(C - I_{12})\Sigma^{-1}\boldsymbol{\beta}_i^{(0)} \right|}{\left\{ (\boldsymbol{\beta}_i^{(0)})'(C - I_{12})\Sigma^{-1}(C - I_{12})\boldsymbol{\beta}_i^{(0)} \right\}^{1/2}}. \quad (13)$$

Let

$$Z_{\max}(\mathbf{y}_{K+1}, \boldsymbol{\beta}^{(0)}, \Sigma) = \max\{Z_1(\mathbf{y}_{1,K+1}, \boldsymbol{\beta}_1^{(0)}, \Sigma), \dots, Z_N(\mathbf{y}_{N,K+1}, \boldsymbol{\beta}_N^{(0)}, \Sigma)\}, \quad (14)$$

where $\boldsymbol{\beta}^{(0)} = ((\boldsymbol{\beta}_1^{(0)})', \dots, (\boldsymbol{\beta}_N^{(0)})')'$. Note that under H_0 , we have

$$\frac{(\boldsymbol{\beta}_i^{(0)})'(C - I_{12})\Sigma^{-1}\mathbf{y}_{i,K+1} - (\boldsymbol{\beta}_i^{(0)})'(C - I_{12})\Sigma^{-1}\boldsymbol{\beta}_i^{(0)}}{\left\{ (\boldsymbol{\beta}_i^{(0)})'(C - I_{12})\Sigma^{-1}(C - I_{12})\boldsymbol{\beta}_i^{(0)} \right\}^{1/2}} \sim N(0, 1)$$

for $i = 1, \dots, N$. Thus, under H_0 and for $z > 0$, we have

$$P(Z_{\max}(\mathbf{y}_{K+1}, \boldsymbol{\beta}^{(0)}, \Sigma) < z) = [2\Phi(z) - 1]^N,$$

where $\Phi(\cdot)$ is the standard normal cumulative distribution function. For a given significance level α , the rejection region is given by

$$\{Z_{\max}(\mathbf{y}_{K+1}, \boldsymbol{\beta}_0, \Sigma) \geq z_{(1 + \sqrt[1-\alpha]{1-\alpha})/2}\}, \quad (15)$$

where $z_{(1 + \sqrt[1-\alpha]{1-\alpha})/2}$ is the $((1 + \sqrt[1-\alpha]{1-\alpha})/2)$ th quantile of $N(0, 1)$, i.e., $\Phi(z_{(1 + \sqrt[1-\alpha]{1-\alpha})/2}) = (1 + \sqrt[1-\alpha]{1-\alpha})/2$.

Because the number of years K is generally small, we also seek to account for the variability in the estimates of $\boldsymbol{\beta}_i$ and Σ . Therefore, we adopt a noninformative Jeffrey's-type prior distribution, namely,

$$\pi(\boldsymbol{\beta}, \Sigma) \propto |\Sigma|^{-1/2} \quad (16)$$

In combination with the likelihood, this gives the posterior distribution

$$\pi(\boldsymbol{\beta}, \Sigma | D_K) \propto \Sigma^{-(KN+1)/2} \exp \left\{ -\frac{1}{2} \sum_{k=1}^K \sum_{i=1}^N (\mathbf{y}_{ik} - \boldsymbol{\beta})' \Sigma^{-1} (\mathbf{y}_{ik} - \boldsymbol{\beta}_i) \right\} \quad (17)$$

We sample from this sequentially, with

$$\boldsymbol{\beta}_i | \Sigma \sim N(\hat{\boldsymbol{\beta}}_i, \Sigma/K), \quad i = 1, \dots, N \quad (18)$$

$$\Sigma^{-1} \sim \mathcal{W}(\Psi^{-1}, NK - 12) \quad (19)$$

$$\Psi = \sum_{k=1}^K \sum_{i=1}^N (\mathbf{y}_{ik} - \boldsymbol{\beta}_i)(\mathbf{y}_{ik} - \boldsymbol{\beta}_i)' \quad (20)$$

where $\mathcal{W}(\Psi, \nu)$ is a Wishart distribution with scale matrix Ψ and ν degrees of freedom.

This yields the following algorithm for online monitoring of the proportional usage data.

Yearly Monitoring Algorithm

Step 0 Set significance level α

Step 1 Compute credible level γ_α

- For each of M replicates, perform the following simulations:
 - Simulate new data $\mathbf{y}_{i,K+1}^{*(m)} \sim N(\hat{\boldsymbol{\beta}}_i, \hat{\Sigma})$ independently for $i = 1, \dots, N$
 - Perform B_1 replicates of the following simulation:
 - (i) Generate $\boldsymbol{\beta}_{mb}^{(0)}$ and Σ_{mb} from the “posterior” distribution

$$\pi(\boldsymbol{\beta}^{(0)}, \Sigma | D_K) \propto \Sigma^{-(KN+1)/2} \exp \left\{ -\frac{1}{2} \sum_{k=1}^K \sum_{i=1}^N (\mathbf{y}_{ik} - \boldsymbol{\beta}_i^{(0)})' \Sigma^{-1} (\mathbf{y}_{ik} - \boldsymbol{\beta}_i^{(0)}) \right\}. \quad (21)$$

- (ii) Calculate the indicator function

$$\delta_b(\mathbf{y}_{K+1}^{*(m)}, \boldsymbol{\beta}_{mb}^{(0)}, \Sigma_{mb}) = \mathbb{1} \left\{ Z_{\max}(\mathbf{y}_{K+1}^{*(m)}, \boldsymbol{\beta}_{mb}^{(0)}, \Sigma_{mb}) \geq z_{(1 + \sqrt{1-\alpha})/2} \right\}, \quad (22)$$

where $\mathbf{y}^{*(m)} = ((\mathbf{y}_{1,K+1}^{*(m)})', \dots, (\mathbf{y}_{N,K+1}^{*(m)})')'$ for $b = 1, \dots, B_1$.

- Calculate $\hat{q}_m = \frac{1}{B_1} \sum_{b=1}^{B_1} \delta_b(\mathbf{y}_{K+1}^{*(m)}, \boldsymbol{\beta}_{mb}^{(0)}, \Sigma_{mb})$.

for $m = 1, \dots, M$.

- Compute γ_α as the α th percentile of the empirical distribution of the M values of \hat{q}_m 's.

Step 2 Monitor

- Using the observation \mathbf{y}_{K+1} in the $K + 1$ year, perform B_2 replicates of the following:
 - (i) Generate $\boldsymbol{\beta}_b^{(0)}$ and Σ_b from the “posterior” distribution

$$\pi(\boldsymbol{\beta}^{(0)}, \Sigma | D_K) \propto \Sigma^{-(KN+1)/2} \exp \left\{ -\frac{1}{2} \sum_{k=1}^K \sum_{i=1}^N (\mathbf{y}_{ik} - \boldsymbol{\beta}_i^{(0)})' \Sigma^{-1} (\mathbf{y}_{ik} - \boldsymbol{\beta}_i^{(0)}) \right\}. \quad (23)$$

- (ii) Calculate the indicator function

$$\delta_b(\mathbf{y}_{K+1}, \boldsymbol{\beta}_b^{(0)}, \Sigma_b) = \mathbb{1} \left\{ Z_{\max}(\mathbf{y}_{K+1}, \boldsymbol{\beta}_b^{(0)}, \Sigma_b) \geq z_{(1+\sqrt{1-\alpha})/2} \right\} \quad (24)$$

for $b = 1, \dots, B_2$.

- Calculate $\hat{q} = \frac{1}{B_2} \sum_{b=1}^{B_2} \delta_b(\mathbf{y}_{K+1}, \boldsymbol{\beta}_b^{(0)}, \Sigma_b)$.
- If $\hat{q} \geq \gamma_\alpha$, do not reject H_0 , i.e., no abnormal consumptions in the $K + 1$ year.
- If $\hat{q} < \gamma_\alpha$, reject H_0 , and report that there are abnormal logit transformed yearly proportional consumptions for at least one account, which corresponds to account i^* such that

$$i^* = \operatorname{argmax}_{1 \leq i \leq N} \{ Z_i(\mathbf{y}_{i,K+1}, \hat{\boldsymbol{\beta}}_i, \hat{\Sigma}) \}.$$

4.4 Comparison of Model-Free and Model-Based Monitoring Procedures

A feature of the transformation in Equation 5 is that it applies separately to each of the 12 months of the year. This contrasts with the more traditional multiple logistic transformation that would express each of 11 months relative to a 12th, benchmark month, which omits one month in order to enforce the constraint that the 12 proportions sum to unity. As we observe in the boxplot-based method, a substantial shift in the consumption

of a single month affects the proportion values for the other 11 months, as well, which introduces complicated dynamics in the relative behavior of the overall proportion vector. Expressed in the diagonal matrix C , this chaotic behavior would require search over a large space of possible values of C to elaborate the wide range of possible distortions across the 12 monthly proportions.

Our method is far simpler, and far more interpretable: for a given month m in a given account i , the alternative hypothesis specifies a multiplicative increase in the log odds of the proportion p_{ikm} . A disadvantage of this approach is that it is not the case that the inverse-logit transformed proportions sum to 1, but the benefit is interpretability of the change in a given month's proportion. Additionally, this approach also sidesteps the possibility for chaotic behavior across the full proportion vector \mathbf{y}_{ik} , in favor of a marginal effect within each month that does not directly impact the mean value in other months.

To demonstrate the relative performance of the two monitoring approaches, we proceed with a constructive data analysis. We start with the accounts 1 and 2, identified by the model-free procedure as outliers. We also estimate the full statistical model across $K = 5$ years.

Suppose we know *a priori* that a given series i is an outlier in the sense of being out-of-control in a given year. Within the model, this means, the mean value of the new year ($K + 1$) is $C\beta_i$. Under H_1 , we can calculate the effective nominal increase in magnitude for a given month m as $\hat{C}_{im} = y_{i(K+1)m}/\beta_{im}$. The accounts with large values along the diagonal of \hat{C} are of intuitive interest, so we consider two more accounts. First, we calculate the sum of the squared diagonal for the full matrix \hat{C}_i , namely, $\sum_{m=1}^{12} \hat{C}_{im}^2$, and consider the account with the large such value. For the second account, we apply the same procedure to the subset of indices m that correspond to the months October–April.

These four accounts are shown in Figure 8. In the top panel, we plot the fitted mean value based on $\hat{\beta}_i$ on the proportional scale, as well as the new data observation \mathbf{y}_i . For reference, the historical data is shown in gray. The second row shows the same data, transformed to the logit scale. Finally, the bottom row shows the ratio of $\mathbf{y}_{i(K+1)}$ to $\hat{\beta}_i$, which can be thought of as the nominal proportional increase \hat{C}_i of the new observation to its mean, the most direct estimate of the true change from the in-control value.

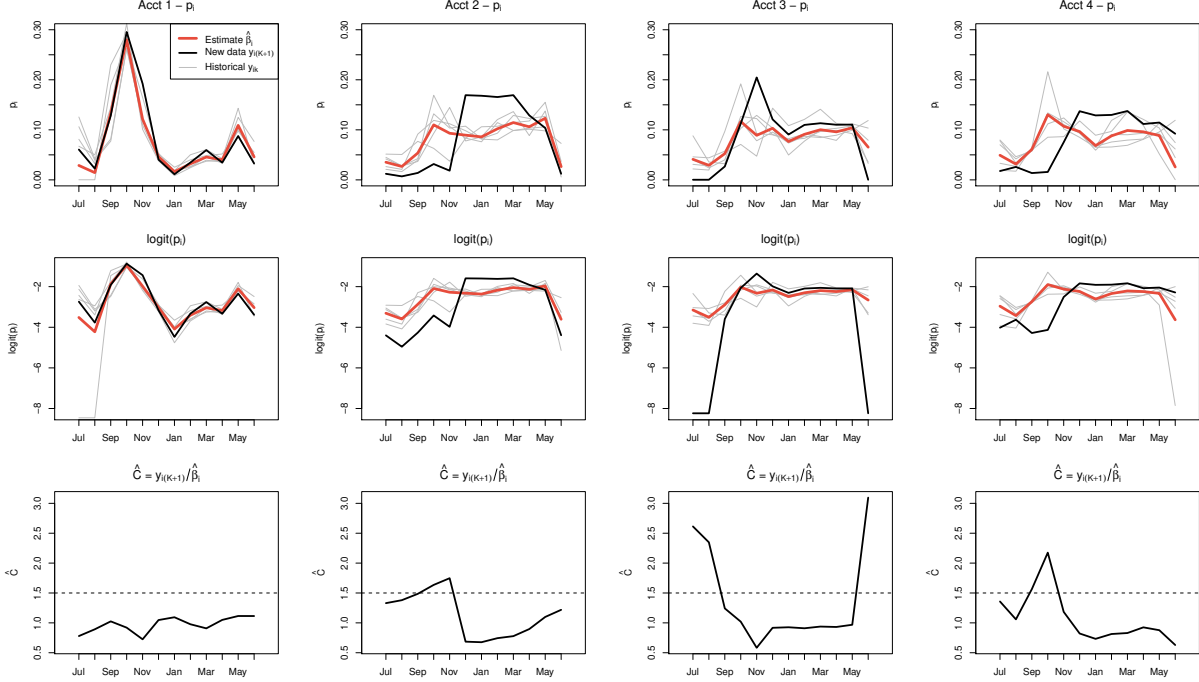


Figure 8: *Top*: Monthly proportional energy consumption p_i for four accounts, accounts 1 and 2 identified using the model-less approach, and accounts 3 and 4 identified as exhibiting the largest ratio $\hat{C}_i = \sum_{m=1}^{12} y_{i(K+1)m} / \hat{\beta}_{im}$ across all the data (account 3) and across only the months October–April (account 4). Shown are in-control historical proportions and logit-transformed mean value. Hypothesis testing is performed for the single new observation in period $(K + 1)$, or 2017–2018. *Middle*: Monthly logit-scale proportional usage values, showing estimated mean value and corresponding transformed data y_i for each account. Estimation and hypothesis tests are performed on these transformed data points. *Bottom*: Empirical increase in monthly consumption in year $(K + 1)$ as a percent of the mean value. Noted is the threshold $C = 1.5$, which reliably identifies large deviations from the mean value.

As noted, the first two accounts in Figure 8 were identified using the model-free procedure. Two scenarios are present: the new observation in period $(K + 1)$ is consistent with past behavior, as in the first account, and the model-free method likely identified the outlier based on deviations from the group-wide trends. In the second account, the observation in the new period exhibits substantial differences from the historical trend. Accordingly, the first example is not likely to be well-suited to identification with the model-based approach.

The figure also shows the transformed values of the proportions on the logit scale, as well as the empirical estimates of \hat{C} for both accounts. For the first account, we see a stable ratio of observed, new values to the estimates based on historical data, and none

of the ratios is much larger than 1. On the other hand, the second account exhibits a sharp increase in the mean parameter associated with November. The magnitude is large at over 1.5, and this is an intuitively appealing value. Moreover, the second is of the type of outlier the model is well-suited to identify: the new observation is not consistent with past behavior during the cold months, from November to March. The decrease in November may reflect the increase in December, a nonlinear relationship that is difficult to specify in terms of the matrix \mathbf{C} . Nonetheless, the empirical estimates suggest a clear discontinuity between the current observation and estimates based on its past behavior.

We do note that the first outlier account exhibits a one historical series with low numerical stability: in one year, July and August both exhibited very low consumption in that account, and this is exaggerated by the logit transformation into a very large, negative value. The estimation procedure itself is robust to this large observation, and the estimate for that month is only somewhat influenced by these outliers.

In the first of the remaining two accounts, we observed large values of \hat{C}_i , but they occur in the edge months of July, August, and June. Although the magnitude is substantial, the real proportion of usage is quite small in these months. Although the differences may be statistically large, these deviations are not practically significant—they do not appear to reflect major behavioral changes in the series’ yearly proportional pattern, so much as artifacts of the logit transformation. This suggests that, in order for the model-based approach to work, we should monitor for changes of magnitude around $c = 1.5$ in magnitude, only in the winter months.

Therefore, we can draw two conclusions on the basis of the visual representation. First, the model-based procedure can capture significant, out-of-control behavior, in terms of the estimated ratio \hat{C} . However, the types of out-of-control behavior come with caveats: we require an explicit magnitude C of change in the mean parameters β_i , we should only consider specific months, and the we must calibrate the values of all 12 diagonal elements C_m to accommodate a change of specific magnitude in only one month. Similar exercises are necessary for changes in each of the other months that may be of interest.

Second, we observe that the model-based approach has low power to identify patterns in the proportions wherein a single account exhibits behavior out-of-sync with other, similar

accounts. The grouping structure is only employed in the model-based approach to account for low sample sizes, and pool estimation of the variance. The model itself does not capture deviations in single accounts from their group-wise trends.

Despite its comparative simplicity, the model-free approach requires far fewer assumptions, and identifies a wider range of out-of-control behaviors in the data.

Because of small sample sizes, the model-based approach requires more detailed specification of the full scenarios, and the grouping of similar accounts is a necessary component of the model to permit pooling of information. But, this will only increase precision on estimates of individual accounts’ mean profiles, which may miss accounts that deviate from group-wise patterns not captured by an account-level model.

5 Statistically Clustering to Identify Homogeneous Groups

Groups

For accounts such as those in Apartment Complex A, the homogeneous behavior we observe in the data reinforces known structural similarities between the accounts. But, in cases such as the single account of service type “seasonal - commercial” in Table 2, such a grouping is unavailable. To this end, we also sought a statistical method to group accounts with similar behavior. This would be followed by flagging anomalous accounts and / or times using methods similar to Section 4. We describe hierarchical clustering based on the intra-year proportions introduced in Section 4.

We constructed fiscal year proportions for 233 accounts, removing one account with a negative observation; three accounts with missing observations; and one account in Apartment Complex B that is primarily 0. We considered two years of data, fiscal years 2016–2018. We computed the Euclidean distances between accounts based on 24 data points, under the assumption they are independent. For two vectors of 24 proportions (two years of proportions), \mathbf{p}_i and \mathbf{p}_j , $i \neq j$, we calculated the distances $d(\mathbf{p}_i, \mathbf{p}_j) = \sqrt{\sum_{k=1}^{24} (p_{ik} - p_{jk})^2}$

We then applied hierarchical clustering (Johnson et al., 2002). We used Ward’s method to cluster the accounts (Ward Jr, 1963), which minimizes the error sum-of-squares when agglomerating clusters. To select the number of clusters, we used the silhouette criterion.

This offers a conventional procedure for identifying the number of clusters in a set of data by using the tightness of groups of observations to determine the optimal number of groups (Rousseeuw, 1987).

We first applied the clustering to the residential utility accounts, as defined in Section 2 but with some series removed, as previously discussed in this section. We considered 69 accounts in Apartment Complex A and 11 accounts in Apartment Complex B. The clusters are shown in Figure 9. In particular, cluster 1 consists of 23 accounts from Apartment Complex A, while cluster 2 contains all of Apartment Complex B accounts and the remaining 46 accounts in Complex A. The clusters are distinguished by comparatively high usage in June in cluster 1 and a smoother overall pattern during the academic year, and high November usage in cluster 2 with a greater decrease in January.

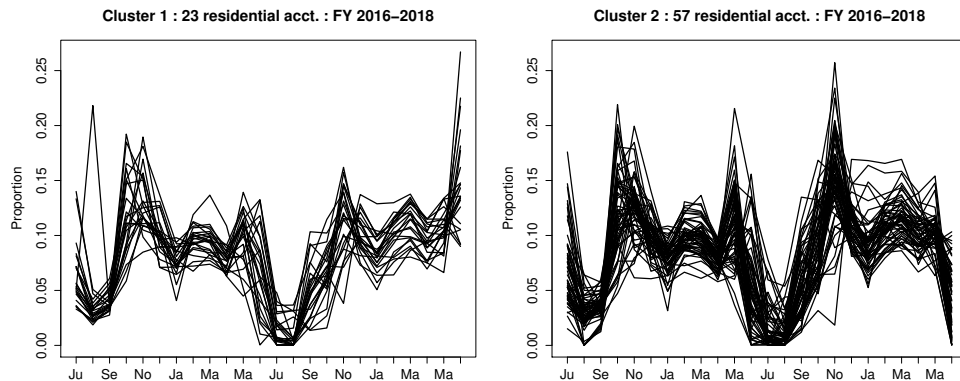


Figure 9: Fiscal-yearly proportion vectors for clustered residential accounts (Apartment Complexes A and B).

To cluster the non-residential accounts, we used the service groups defined in Table 2, namely, small and medium-to-large accounts. Within each of these groups, we performed hierarchical clustering. We combined the partitions of all non-residential accounts, defined in terms of the account size and the two clusterings. Finally, we combined all degenerate singleton clusters.

The medium-to-large accounts were found to have seven clusters, two of which were degenerate, and the small accounts contained three clusters, one of which was degenerate. This yielded the final eight clusters shown in Figure 9. In addition to the visual homogeneity of these groups, we report in Table 4 the cluster assignment counts for all non-residential

accounts for buildings containing more than one account. We note the grouping of accounts according to the known building labels, in general, such as Apartment Complex F and Apartment Complex E, Building 4.

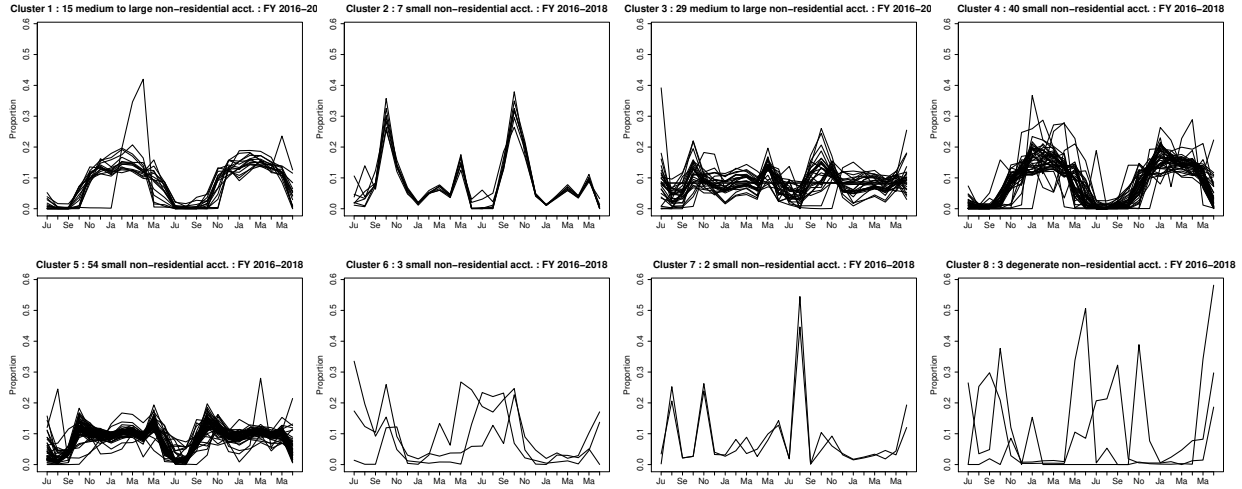


Figure 10: Cluster partition of utility-designated “non-residential” accounts.

	1	2	3	4	5	6	7	8
Ag 1	-	-	-	1	1	-	-	-
Ag 2	1	-	-	1	-	-	-	-
Dormitory 1	-	-	-	-	-	1	1	-
Student Union	-	-	2	-	-	-	-	-
Dormitory 2	-	-	2	-	1	-	-	-
Dormitory 3	-	-	-	-	7	-	-	-
Apartment Complex C	-	-	7	-	-	-	-	-
Apartment Complex D	-	-	4	-	3	-	-	-
Apartment Complex E, Bldg. 1	-	-	-	-	8	-	-	-
Apartment Complex E, Bldg. 2	-	-	-	1	7	-	-	-
Apartment Complex E, Bldg. 3	-	-	-	-	8	-	-	-
Apartment Complex E, Bldg. 4	-	-	-	-	12	-	-	-
Apartment Complex F	-	-	1	20	-	-	-	-

Table 4: Cluster assignment for utility-designated “non-residential” accounts.

Within each of the homogeneous clusters, we then used the approach of Section 4. Under this procedure, we identify possible anomalies across all accounts, even those for which known homogeneous structure is unavailable.

6 Implementation for Management

Having specified a method for anomaly detection among fiscal yearly proportions, the final steps are implementation, integration into the Facilities Operations energy management workflow, and a mechanism to incorporate feedback from engineers into the statistical model. We pursued seamless interaction between the Department of Statistics and Facilities Operations through an intense collaboration on a weekly, or even more frequent, basis. These meetings occurred face-to-face as well as electronically, and provided opportunities for dynamic exchange of ideas.

Implementation requires, on the one hand, aggregation, storage, and analysis of the data; and on the other hand, an interface with which Facilities Operations may review the results of the anomaly detection as well as manage the information provided by the analysis.

Data management and analysis proceed from records of monthly utility usage, in terms of the specific dataset discussed above, as well as a suite of additional datasets collected on separate utility services including electric, water, and sewage. We implemented an automated software procedure to periodically download data from a state-wide reporting system used to track state utility records. After extracting utility data via a web API, we store inputs and outputs in a database server. We also integrated into the same database system those datasets not yet available through the web-based procedure. The procedures were hosted on a Linux server and backed by a Microsoft SQL Server database. We implemented the automation procedures in a combination of shell scripts, Python, and R. These procedures included automatic merging of the utility data with NOAA weather data, normalization and degree day-adjustment, and the analysis detailed in the previous sections. A basic flow diagram of the various inputs is shown in Figure 11.

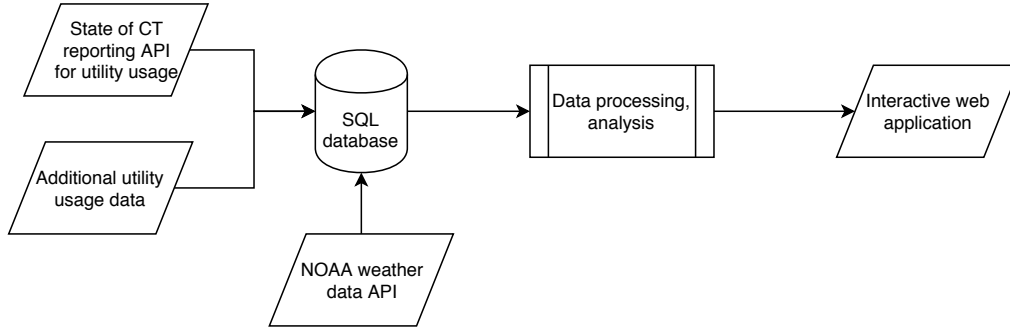


Figure 11: Flow diagram of data ingestion, storage, processing, and presentation to operators.

Following the pre-processing and analysis steps, we provided a web interface for dynamic interaction with the data and statistical outputs. These primarily consisted of a database with a record of which utility accounts were flagged as anomalous, which Facilities Operations engineers interact with through a dashboard interface implemented in R Shiny (Chang et al., 2018). This software implementation provides professional-quality, contemporary web technology, as well as back-end implementation that may be managed, customized, and extended by statisticians who were not previously trained in web development. We implemented the flagging system in such a way that Facilities Operations may dismiss flags after review of the physical facilities, which was recorded in the database. The cluster results of the flagging interface are shown in Figure 12.

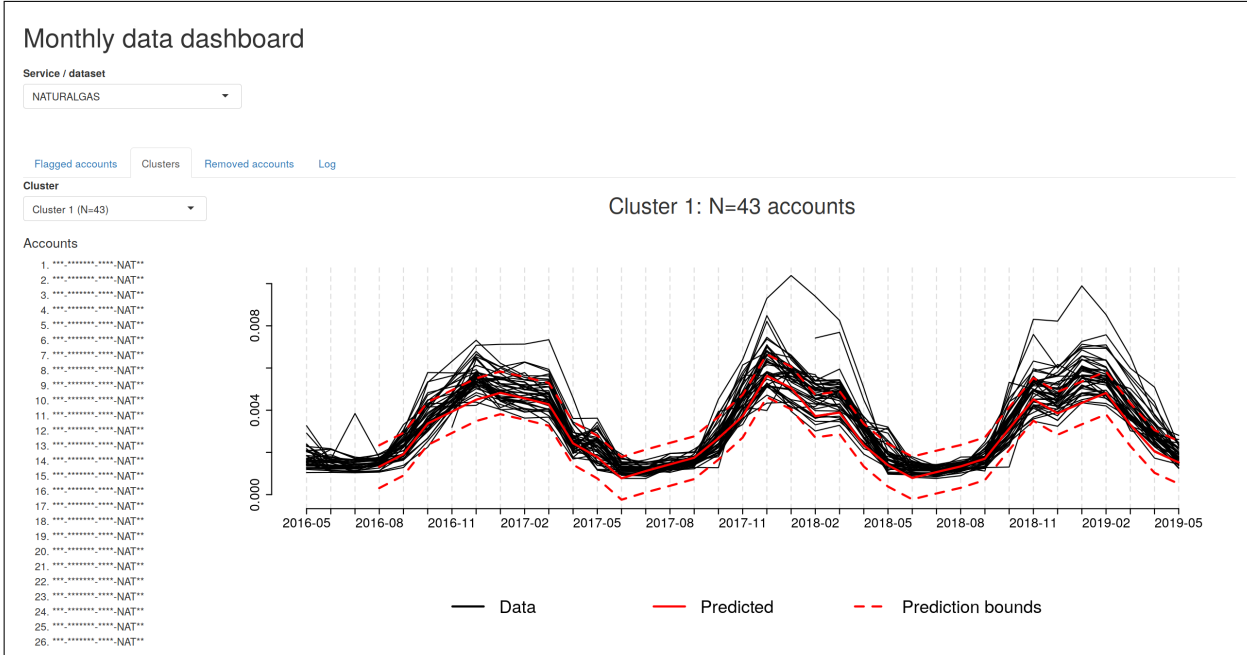


Figure 12: Cluster analysis output for flagged accounts. Account names and numbers are redacted for privacy purposes.

Aside from interaction with the flagging system, the primary mechanism for operator feedback is through the composition of the homogeneous groups to which the boxplots based analyses are applied. Although the cluster analysis provides a good option in the absence of operator-derived groupings, it is improved by operation in tandem with the extensive domain experience of the Facilities Operations engineers. Therefore, Statistics and Facilities Operations can work in tandem to review and verify the validity of the groupings, as well as the sensibility of the resultant analysis. In some instances, such as the laundry dryer in Apartment Complex A, Building 3, it is necessary to manually adjust even the known homogeneous groups to more accurately reflect the ground truth of similarity in energy consumption profiles of accounts in the same group.

7 Discussion

We have described the development and implementation of easy to understand statistical methods in an applied context. The tools and approaches described in this article offer a useful framework for analyzing and monitoring energy usage on a university campus through

an ongoing collaboration between members of the Statistics Department and Facilities Operations staff. The energy monitoring has enabled us to gain deeper insight into energy usage at specific sites of interest and identify potential problems without requiring extensive manual searches. An attractive characteristic of this project is that an academic department in an R1 institution has coordinated a long-term problem solving collaboration with the university's administrative units.

We have proposed both a model-free graphical procedure for detecting anomalous values for monthly energy usage as well as for monthly proportions within a given year. We have also formulated a simple model-based approach in the Bayesian framework which is useful even with small sample sizes. These approaches have been automated and can also be easily modified for similar operational problems that can benefit from applying simple and informative statistical methods to a large number of observational units. Our project showcases well-informed statistical practice in collaboration with non-technical collaborative counterparts.

Acknowledgements

The authors would like to thank the Utility Operations & Energy Management team at Facilities Operations, especially Mark Bolduc and Brian McKeon for their time, for their time, resources, and expertise. We would like to thank the Editor, the Associate Editor, and two reviewers for their helpful comments and suggestions, which led to an improved version of the paper.

References

Breyer, A., Etter, D., Friedrichs, M., Guerriero, R., Ho, M. N., and Kerns, N. (Published 2011. Accessed July, 2020). Assessing a campus energy monitoring system. <http://graham.umich.edu/media/files/campus-course-reports/CEMS%20Final%20Report.pdf>.

- Chang, W., Cheng, J., Allaire, J., Xie, Y., and McPherson, J. (2018). *shiny: Web application framework for R*. R package version 1.2.0.
- Cruz Rios, F., Naganathan, H., Chong, W. K., Lee, S., and Alves, A. (2017). Analyzing the impact of outside temperature on energy consumption and production patterns in high-performance research buildings in arizona. *Journal of Architectural Engineering*, 23(3):C4017002.
- Fu, Y. and Jeske, D. R. (2014). Spc methods for nonstationary correlated count data with application to network surveillance. *Applied Stochastic Models in Business and Industry*, 30(6):708–722.
- Johnson, R. A., Wichern, D. W., et al. (2002). *Applied Multivariate Statistical Analysis*. Prentice hall Upper Saddle River, NJ.
- Lieberman, E. (2010). Web-based display tracks campus energy use.
- Little, R. J. and Rubin, D. B. (2019). *Statistical Analysis with Missing Data*, volume 793. Wiley.
- Ma, Y., Lu, M., and Weng, J. (2015). Energy consumption status and characteristics analysis of university campus buildings. In *5th International Conference on Civil Engineering and Transportation*. Atlantis Press.
- Ma, Z., Song, J., and Zhang, J. (2017). A real-time detection method of abnormal building energy consumption data coupled POD-LSE and FCD. *Procedia Engineering*, 205:1657–1664.
- Moritz, S. and Bartz-Beielstein, T. (2017). imputeTS: Time series missing value imputation in R. *The R Journal*, 9(1):207–218.
- O’Hara, C., Hobson-Dupont, M., Hurgin, M., and Thierry, V. (Published 2007, Accessed July, 2020). Monitoring electricity consumption on the WPI campus. <https://web.wpi.edu/Pubs/E-project/Available/E-project-060107-130245/unrestricted/iqpfinaldraft.pdf>.

- Quayle, R. G. and Diaz, H. F. (1980). Heating degree day data applied to residential heating energy consumption. *Journal of Applied Meteorology*, 19(3):241–246.
- Rashid, H. and Singh, P. (2018). Monitor: An abnormality detection approach in buildings energy consumption. In *2018 IEEE 4th International Conference on Collaboration and Internet Computing (CIC)*, pages 16–25. IEEE.
- Rousseeuw, P. J. (1987). Silhouettes: a graphical aid to the interpretation and validation of cluster analysis. *Journal of Computational and Applied Mathematics*, 20:53–65.
- Seem, J. E. (2007). Using intelligent data analysis to detect abnormal energy consumption in buildings. *Energy and buildings*, 39(1):52–58.
- Ward Jr, J. H. (1963). Hierarchical grouping to optimize an objective function. *Journal of the American Statistical Association*, 58(301):236–244.
- Zhao, L. (2014). A novel method for detecting abnormal energy data in building energy monitoring system. *Journal of Energy*.